2021 43rd Annual International Conference of the
IEEE Engineering in Medicine & Biology Society (EMBC)
Oct 31 - Nov 4, 2021. Virtual Conference

The Influence of Spatial Smoothing Kernel Size on the Whole-brain Dynamic Functional Network Connectivity and Meta-state Parameters

Behnaz Jarrahi, *Member, IEEE*

Abstract— **In functional magnetic resonance imaging (fMRI), spatial smoothing procedure is generally a stable step in the preprocessing stream. Previous research (including ours) suggested dependency of the static functional connectivity on the size of the spatial smoothing kernel size. But its impact on the time-varying patterns of functional connectivity has not been investigated. Here, we sought to identify the effects of spatial smoothing on brain dynamics by performing dynamic functional network connectivity (dFNC) and meta-state analysis, a unique approach capable of examining a higher-dimensional temporal dynamism of whole-brain functional connectivity. Gaussian smoothing kernel with different widths at half of the maximum of the height of the Gaussian (4, 8, and 12 mm FWHM) were used during preprocessing prior to the group independent component analysis (ICA) with a relatively high model order of 75. dFNC was conducted using the sliding-time window approach and k-means clustering algorithm. Meta-state dynamics method was performed by reducing the number of windowed FNC correlations using principal components analysis (PCA), temporal and spatial ICA and k-means. Results revealed robust effects of spatial smoothing on the connectivity dynamics of several network pairs including a variety of cognitive/attention networks in a connectivity state with the highest occurrence (FDR corrected-$p < 0.01$). Meta-state analyses indicated significant changes in meta-state metrics including the number of meta-states, meta-state changes, meta-state span, and the total distance. These changes were particularly pronounced when we compared resting state data smoothed with 8 vs. 12 mm FWHM. Our preliminary findings give insights into the effects of spatial smoothing kernel size on the dynamics of functional connectivity and its consequences on meta-state parameters. It also provides further indication of the importance of evaluating variance associated with preprocessing steps on analysis outcomes.**

I. INTRODUCTION

In blood oxygenation level-dependent (BOLD) functional magnetic resonance imaging (fMRI), acquired images generally require some preprocessing prior to analysis [1]. One common procedure is spatial smoothing, which usually involves convolving the BOLD signals with a Gaussian function of a specific size defined as the Full Width at Half Maximum (FWHM) [1]. Previous studies that investigated the impact of spatial smoothing on region of interest (ROI) or at network levels at rest and during a task [2], have shown dependency of static functional connectivity on smoothing kernel sizes. A more recent study examined the spatial smoothing effects on independent component analysis (ICA)-based task fMRI data and found an increase in the functional coupling strengths with spatial smoothing [3]. We found a similar result in resting-state ICA (forthcoming).

B. Jarrahi is with the Department of Anesthesia, Stanford University, CA, USA; (email: behnaz.jarrahi@stanford.edu).

Up to the present, the influence of spatial smoothing on the dynamic functional network connectivity (dFNC) of ICA-derived intrinsic connectivity networks (ICNs) have not been studied. In this study, we aim to examine the dFNC and meta-state metrics to investigate how smoothing kernel size impact brain dynamics. By introducing a higher-dimensional state space, the meta-state approach allows complex states to overlap in time, thus enabling the estimation of different measures of neural dynamism [4]. We hypothesized that application of different smoothing kernel sizes during preprocessing would influence the higher-dimensional temporal dynamism of functional connectivity by modifying the resultant windowed connectivity patterns.

II. MATERIALS AND METHODS

A. Data Acquisition and Preprocessing

Resting state fMRI data were collected from 22 healthy volunteers (12 females, mean age 37.73 years) on a 3.0T GE scanner using EFGRE3D pulse sequence (TR/TE = 2000/30 ms, FOV = 220×220 mm^2 acquisition matrix = 64×64, flip angle = 76^o, slice thickness = 4 mm, 31 slices). All MRI scans were performed when subjects were relaxed with their eyes closed. Informed consent was obtained in accordance with the local institutional review board approved protocol. All data passed the strict MR image quality criteria (mean framewise displacement of head < 0.2 mm). Data were preprocessed with SPM12 (Wellcome Trust Centre for Neuroimaging, UK) in a series of steps commonly used in the field [1]. This included slice time and motion correction, coregistration, and spatial normalization into the Montreal Neurological Institute coordinates. Spatial smoothing with an isotropic Gaussian kernel FWHM 4, 8, and 12 mm were applied. 8 mm FWHM was chosen as it is the typical value used in group ICA of fMRI studies. 4 and 12 mm FWHM were chosen as arbitrary low and high smoothing values.

B. Group Independent Component Analysis

Group ICA with 75-IC decomposition was performed using the GIFT toolbox (University of New Mexico, USA) following a well-established ICA resting state methodology [5]. ICNs were identified based on the methodology recommended by Allen et al. [5], [6]. 40 ICNs were identified and classified into one of visual (VN), auditory/language (AUD/LN), sensorimotor (SMN), basal ganglia (BG), cognitive and attention (CAN), default mode (DMN), subcortical (SCN), Brain stem (BSN), and cerebellar (CBN) networks (Fig. 1). The resultant ICNs are very similar to those found in previous ICA studies [5]–[9].

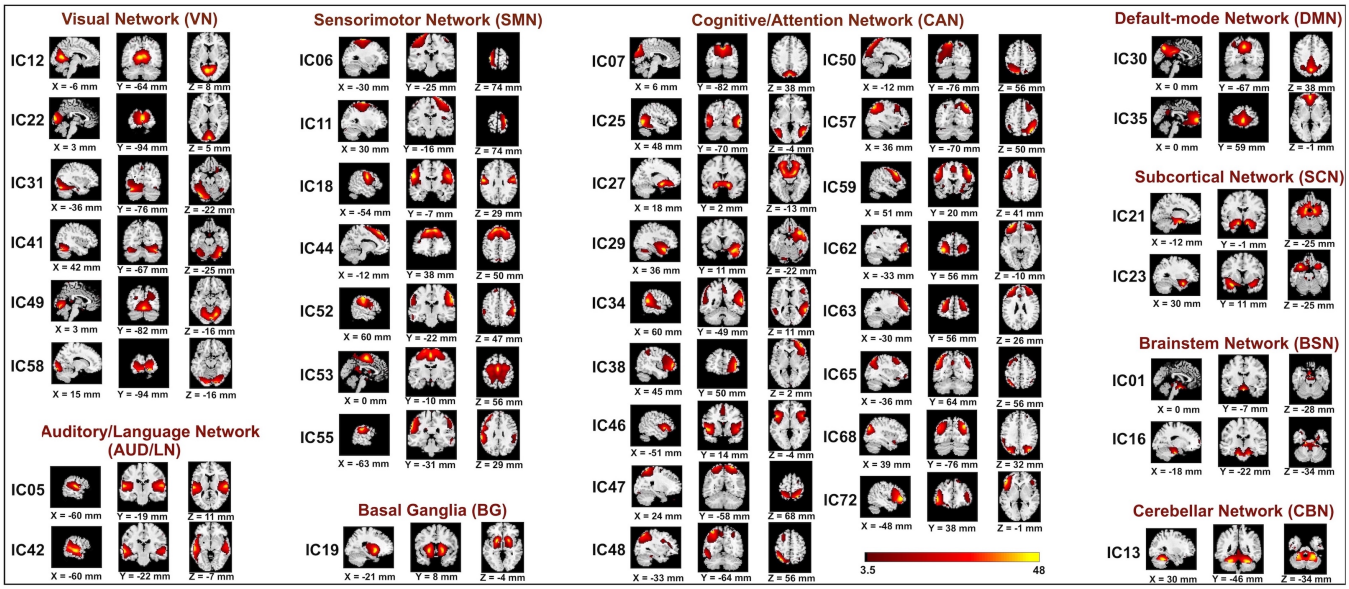

Fig. 1. Spatial maps of 40 ICNs from 75-IC decomposition shown on the three most representative slices in neurological convention (right = right)

C. Dynamic FNC and Meta-state Analyses

ICN time-courses were detrended using a third-order polynomial fit, despiked by replacing outlier time points with third order spline fit to cleaner neighboring points using AFNI's 3dDespike, and filtered using a fifth order Butterworth filter with a passband of 0.01 to 0.15 Hz. Time windows were sub-sampled for each subject and only those with local maxima in functional connectivity variance were selected for further analysis [6]. dFNC was computed using a sliding window approach as described in details in [6]. Briefly, a tapered window was created by convolving a rectangle of width 30 TRs (60 s, TR = 2 s) with a Gaussian function ($\sigma =$, 3 TRs = 3) that slided in steps of 1 TR. Optical number of dFNC clusters was estimated using eight different methods: elbow, gap statistic, Akaïke information criterion (AIC), Bayesian information criterion (BIC), Dunn index, Silhouette, Davies Boulder, and Ray Turi algorithms (Fig 2). Based on the elbow criterion, which is a more common method, the optimum number of cluster centroids (dynamic connectivity states) was set to 4. K-means clustering with cosine for distance method was applied to windowed covariance matrices. To investigate dFNC differences between conditions, median of dFNC correlations across windows were used [6], [9], and differences in dynamic correlation patterns were evaluated using a paired t-test set at $p < 0.01$ corrected for multiple comparisons using the false discovery rate (FDR). Comparison of correlation was only conducted if there were subjects with finite correlations for a given cluster state in each condition [6].

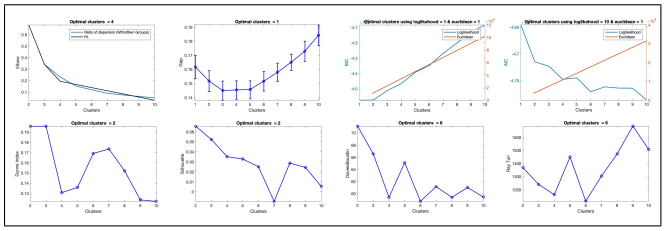

Fig. 2. dFNC optimal number of cluster estimation

Meta-state dynamics method [4] was ran by reducing the number of windowed FNC correlations to 8 clusters using four different methods: k-means, PCA, temporal and spatial ICA (using ICA by entropy bound minimization method; ICA-EBM). dFNC correlations were factorized into the continuous loading coefficients and discretized using quartile discretization. The following metrics were performed and compared using paired t-test set at $p < 0.01$: number of meta-states, changes of meta-states, meta-state span, and the total distance traveled in the n-dimensional state space.

III. RESULTS

The dynamic states obtained from k-means clustering of all datasets with the number of cluster occurrences using 100 bootstrap iterations, as well as frequency of each cluster, mean dwell time in windows and mean of state transition matrix across 22 subjects are displayed in Fig. 3. Different state vectors were observed for data preprocessed with smoothing kernel FWHM 4, 8, and 12 mm (Fig. 4). Cluster mean correlations for each dataset tests and cluster paired t-test results (FDR-corrected $p < 0.01$) are shown in Fig. 5. Results of meta-state analyses are presented in Table 1.

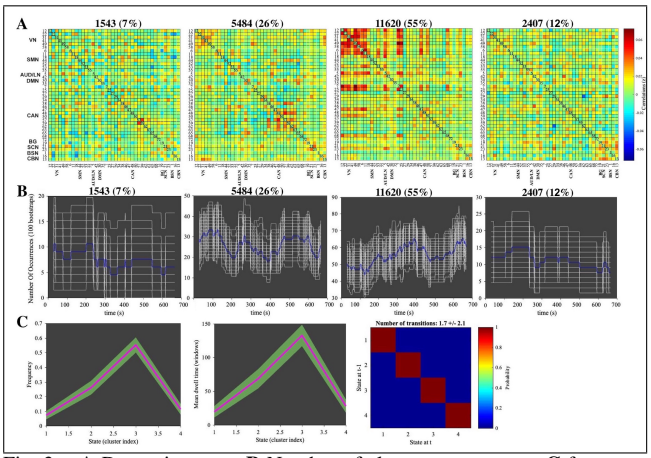

Fig. 3. **A** Dynamic states; **B** Number of cluster occurrences; **C** frequency, mean dwell time, and mean of state transition matrix across subjects.

Table 1. Meta-state Results

S4-S8	Number of States				Change Between States				State Span				Total Distance			
Method	T-value	p-value	Mean of S4	Mean of S8	T-value	p-value	Mean of S4	Mean of S8	T-value	p-value	Mean of S4	Mean of S8	T-value	p-value	Mean of S4	Mean of S8
PCA	-7.931	0.000*	82.500	115.818	-7.230	0.000*	88.500	117.136	-7.508	0.000*	21.682	27.818	-6.735	0.000*	128.591	179.227
Temporal ICA	-7.428	0.000*	99.500	131.546	-7.257	0.000*	102.500	132.909	-7.980	0.000*	22.227	29.046	-7.106	0.000*	141.636	198.955
Spatial ICA	-6.880	0.000*	85.955	113.636	-6.390	0.000*	91.636	115.818	-4.765	0.000*	22.546	28.000	-7.623	0.000*	134.318	180.818
K-means	-2.058	0.052	25.000	35.727	-1.751	0.095	38.864	49.773	-1.985	0.060	8.773	11.318	-1.800	0.086	42.818	55.682
S8-S12	**Number of States**				**Change Between States**				**State Span**				**Total Distance**			
Method	T-value	p-value	Mean of S8	Mean of S12	T-value	p-value	Mean of S8	Mean of S12	T-value	p-value	Mean of S8	Mean of S12	T-value	p-value	Mean of S8	Mean of S12
PCA	-3.860	0.001*	115.818	129.000	-3.905	0.001*	117.136	129.864	-3.770	0.001*	27.818	30.682	-4.236	0.000*	179.227	205.364
Temporal ICA	-3.301	0.003*	131.546	140.136	-3.538	0.002*	132.909	141.455	-2.461	0.023*	29.046	30.500	-2.878	0.009*	198.955	215.682
Spatial ICA	-4.075	0.001*	113.636	125.273	-4.221	0.000*	115.818	126.864	-2.088	0.049*	28.000	29.364	-4.093	0.001*	180.818	203.136
K-means	4.470	0.000*	35.727	28.000	2.959	0.008*	49.773	43.364	2.668	0.014*	11.318	10.000	2.850	0.010*	55.682	48.682
S4-S12	**Number of States**				**Change Between States**				**State Span**				**Total Distance**			
Method	T-value	p-value	Mean of S4	Mean of S12	T-value	p-value	Mean of S4	Mean of S12	T-value	p-value	Mean of S4	Mean of S12	T-value	p-value	Mean of S4	Mean of S12
PCA	-7.752	0.000*	82.500	129.000	-7.780	0.000*	88.500	129.864	-8.131	0.000*	21.682	30.682	-7.087	0.000*	128.591	205.364
Temporal ICA	-7.020	0.000*	99.500	140.136	-7.208	0.000*	102.500	141.455	-7.197	0.000*	22.227	30.500	-6.852	0.000*	141.636	215.682
Spatial ICA	-7.138	0.000*	85.955	125.273	-6.860	0.000*	91.636	126.864	-5.495	0.000*	22.546	29.364	-7.683	0.000*	134.318	203.136
K-means	-0.621	0.541	25.000	28.000	-0.728	0.474	38.864	43.364	-0.905	0.376	8.773	10.000	-0.813	0.425	42.818	48.682

* $p < 0.01$. S4, S8, and S12 are data preprocessed with the spatial smoothing kernels FWHM 4, 8, and 12 mm, respectively.

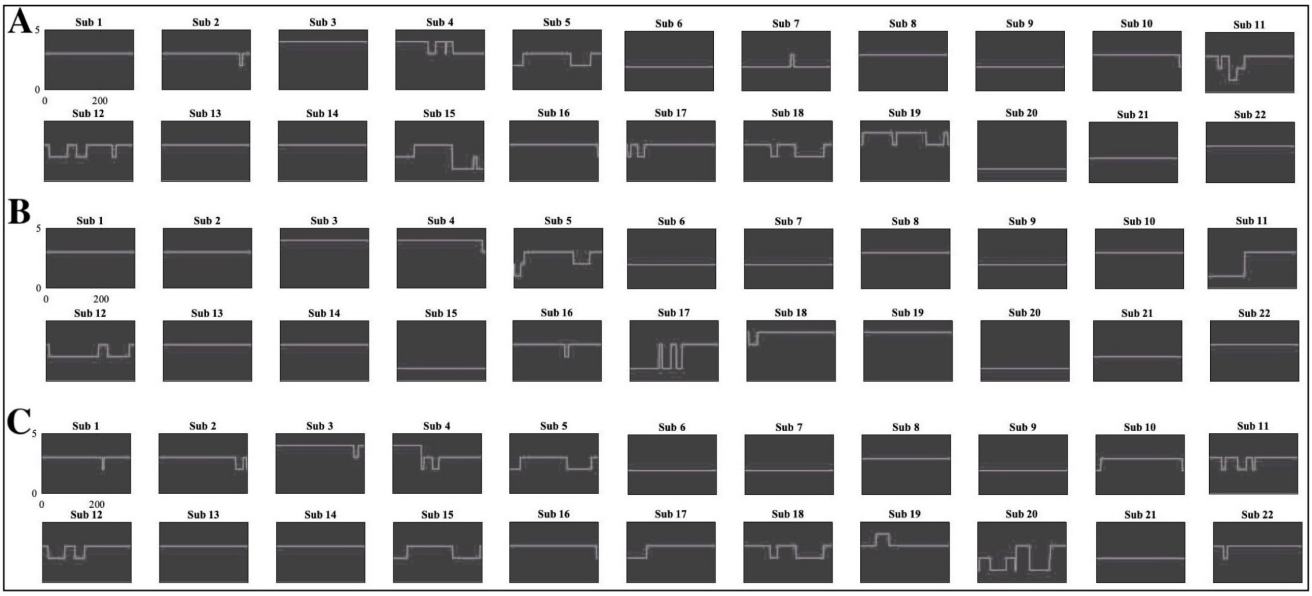

Fig. 4. State vectors for **A** 4 mm, **B** 8 mm, and **C** 12 mm FWHM.

IV. Conclusion

Using a relatively high-level ICA as a data driven technique, we tested the hypothesis of whether changing the spatial smoothing FWHM during preprocessing would influence the dynamics of functional connectivity between large-scale networks in the brain at rest. Our results suggest that dFNC are significantly impacted by the size of the smoothing kernel. Paired t-test at FDR-corrected $p < 0.01$ between datasets with different smoothing kernels indicated robust effects (mostly decrease but also some increase) in the connectivity patterns of almost all ICNs including CANs, DMN, VN, SMN and SCN with a change in smoothing kernel size. These effects were particularly pronounced (with regard to significance and extent) on the dynamic state with highest number of occurrence (i.e., state 3, 55% occurrence) implying probable robust effect on the static FNC (which we analyzed in a separate study). Meta-state analyses with PCA, ICA and k-means all indicated significant changes in all metrics. These findings supplement our knowledge regarding the influence of spatial smoothing on resting-state functional connectivity. Moreover, they provide further indication of the importance of evaluating variance associated with preprocessing steps on analysis outcomes.

References

[1] K. J. Friston, A. P. Holmes, J. Poline, P. Grasby, S. Williams, R. S. Frackowiak, and R. Turner, "Analysis of fmri time-series revisited," *Neuroimage*, vol. 2, no. 1, pp. 45–53, 1995.

[2] T. Alakörkkö, H. Saarimäki, E. Glerean, J. Saramäki, and O. Korhonen, "Effects of spatial smoothing on functional brain networks," *European Journal of Neuroscience*, vol. 46, no. 9, pp. 2471–2480, 2017.

[3] Z. Chen and V. Calhoun, "Effect of spatial smoothing on task fmri ica and functional connectivity," *Frontiers in neuroscience*, vol. 12, 2018.

[4] R. L. Miller, M. Yaesoubi, J. A. Turner, D. Mathalon, A. Preda, G. Pearlson, T. Adali, and V. D. Calhoun, "Higher dimensional meta-state analysis reveals reduced resting fmri connectivity dynamism in schizophrenia patients," *PloS one*, vol. 11, no. 3, p. e0149849, 2016.

[5] E. A. Allen, E. B. Erhardt, Damaraju, *et al.*, "A baseline for the multivariate comparison of resting-state networks," *Frontiers in systems neuroscience*, vol. 5, 2011.

[6] E. A. Allen, E. Damaraju, S. M. Plis, E. B. Erhardt, T. Eichele, and V. D. Calhoun, "Tracking whole-brain connectivity dynamics in the resting state," *Cerebral cortex*, vol. 24, no. 3, pp. 663–676, 2014.

[7] B. Jarrahi and S. Mackey, "Characterizing the effects of mr image quality metrics on intrinsic connectivity brain networks: A multivariate approach," in *2018 40th Annual International Conference of the IEEE Engineering in Medicine and Biology Society (EMBC)*. IEEE, 2018, pp. 1041–1045.

[8] B. Jarrahi and D. Mantini, "The nature of the task influences intrinsic connectivity networks: An exploratory fmri study in healthy subjects," in *2019 9th International IEEE/EMBS Conference on Neural Engineering (NER)*. IEEE, 2019, pp. 489–493.

[9] B. Jarrahi, D. Mantini, U. Mehnert, and S. Kollias, "Exploring influence of subliminal interoception on whole-brain functional network connectivity dynamics," in *2015 37th Annual International Conference of the IEEE Engineering in Medicine and Biology Society (EMBC)*. IEEE, 2015, pp. 670–674.

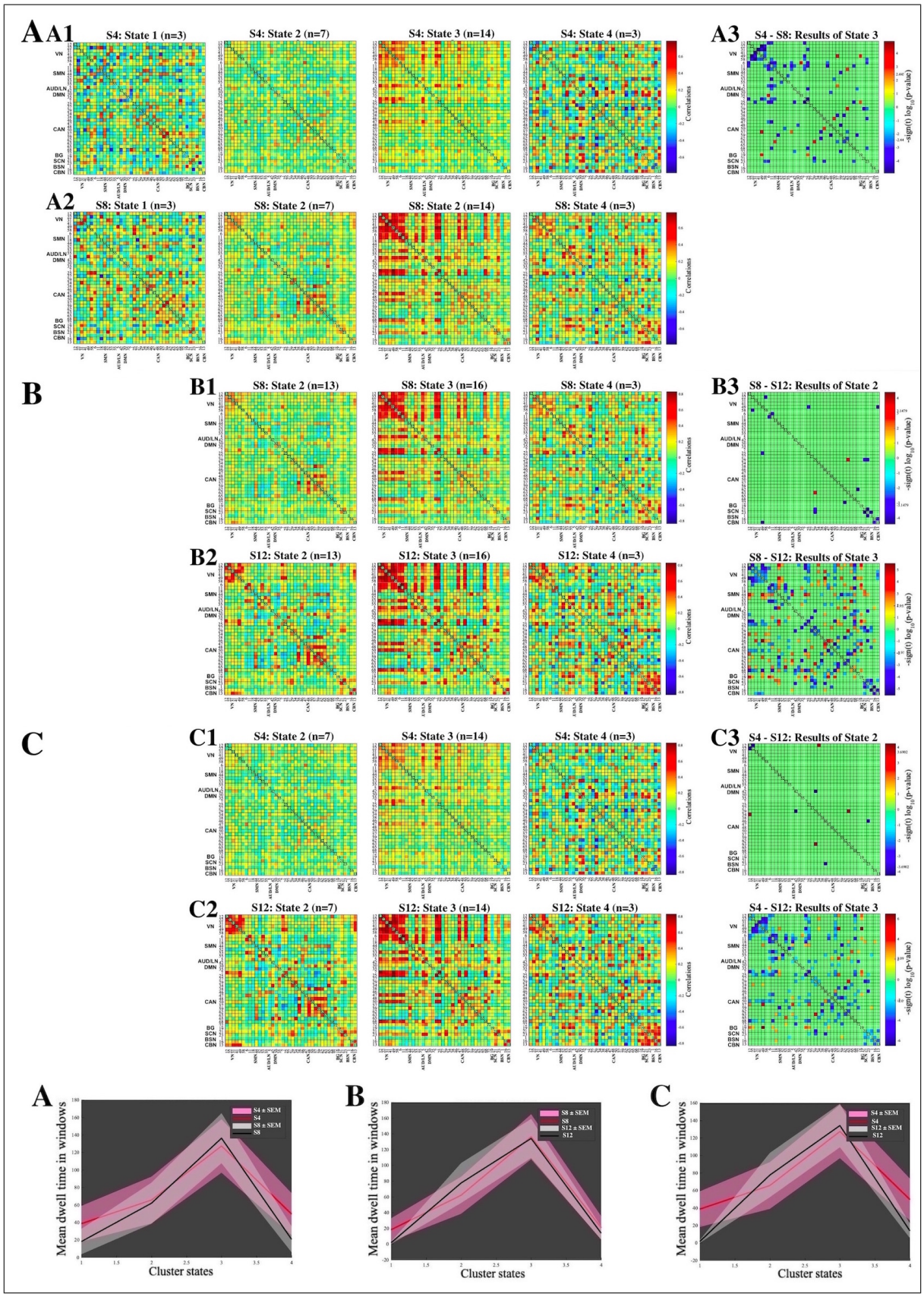

Fig. 5. Significant results showing the effect of smoothing kernel sizes on dFNC corrolations. **A** S4 – S8, **B** S8 – S12, and **C** S4 – S12, where S denotes smoothing kernel FWHM 4, 8, or 12 mm. **A1** Cluster mean correlations of condition S4, **A2** Cluster mean correlations of condition S8, **A3** Cluster paired t-test results of S4 – S8. **B1** Cluster mean correlations of condition S8, **B2** Cluster mean correlations of condition S12, **B3** Cluster paired t-test results of S8 – S12. **C1** Cluster mean correlations of condition S4, **C2** Cluster mean correlations of condition S12, **C3** Cluster paired t-test results of S4 – S12. All results are shown at FDR corrected-$p < 0.01$. Number of subjects with finite correlations (n) is also shown for each condition/state. Mean dwell time vs. cluster states for each tests are shown in the bottom.